Food Chemistry 355 (2021) 129514

Contents lists available at ScienceDirect

Food Chemistry

journal homepage: www.elsevier.com/locate/foodchem

A rapid and sensitive lateral flow immunoassay (LFIA) for the detection of gluten in foods

Robert M. Hnasko *, Eric S. Jackson, Alice V. Lin, Ronald P. Haff, Jeffery A. McGarvey

United States Department of Agriculture, Agricultural Research Service, Pacific West Area, Western Regional Research Center (USDA-ARS-PWA-WRRC), 800 Buchanan St., Albany, CA 94710, United States

ARTICLE INFO

Keywords:
Gluten
Gliadin
Food allergen
Lateral Flow Immunoassay (LFIA)
Monoclonal antibodies
Biosensor

ABSTRACT

The gluten protein found in a variety of cereal grains is a food allergen that can elicit a spectrum of immuno-inflammatory responses in people. Consumer awareness has prompted changes in food labeling requirements, expanded gluten-free food product availability and increased demand for effective gluten testing methodologies. To meet the challenges associated with gluten testing from diverse and complex foods we developed a lateral flow immunoassay (LFIA) using a pair of novel gliadin monoclonal antibodies (MAbs). Using a visual gold reporter, we show sensitive gluten detection (150 ng/mL) from complex food substrates using a fast (<5 min) and easy testing methodology. In this report we characterize the binding properties of a cohort of newly generated gliadin monoclonal antibodies suitable for gluten detection using multiple assay formats and introduce a novel plug-*n*-play test strip platform with integrated test components in a single-use format.

1. Introduction

Undeclared food allergens are a food safety issue and represent >40% of all food product recalls in the U.S. (Gendel & Zhu, 2013; Spotz, 2018). The prevalence of food allergies is rising globally and their economic impact in the U.S. is > $24B annually (Gupta, Holdford, Bilaver, Dyer, Holl, & Meltzer, 2013). Consumer awareness regarding the role of food allergies in health and disease led to the Food Allergen Labeling and Consumer Protection Act that requires declaration of eight food allergens, including gluten, when added as an ingredient (Gupta et al., 2019; Sathe, Liu, & Zaffran, 2016). In 2010, as a part of the Food Safety Modernization Act, the FDA enacted rules for the Preventive Controls for Human Food that required certain manufactures to have allergen control plans to limit cross-contact (Boyce et al., 2010; Gendel, 2013). Additional FDA rules in 2013 were established for food labeling that define < 20 μg/mL as gluten-free (Diaz-Amigo & Popping, 2012; Fierro, Di Girolamo, Marzano, Dahdah, & Mennini, 2017). Gluten is a food allergen that is a mixture of prolamin seed storage proteins found in cereal grains that include wheat, rye and barley (Balakireva & Zamyatnin, 2016). Prolamin gene expression is complex and this results in significant variation in transcribed protein (Wang, Li, Cao, & Zhang, 2020). All prolamins are related and exhibit similar structures that include abundant glutamine and proline residues and repetitive regions (Shewry, 2019; Wieser, 2007). Gluten is a polymeric protein composed of gliadin and glutenin that differ in their solubility and molecular weight with inter- and intra-molecular disulfide bonds that impart the viscoelastic properties of a flour dough (Shewry, 2009; Shewry, Halford, Belton, & Tatham, 2002).

Wheat is an important global food source accounting for 20% of calories consumed by humans (Shewry & Hey, 2015). The abundance and versatility of wheat, and other grains, provide a useful ingredient in many processed food products (Delcour, Joye, Pareyt, Wilderjans, Brijs, & Lagrain, 2012). However, gluten-related disorders afflict 5% of the global population with the most serious being celiac disease (Catassi et al., 2013). This has resulted in a shift by the general population toward the consumption of gluten-free food products as a necessity to manage disease or as a dietary choice (Kulis, Wright, Jones, & Burks, 2015; Valenti, Corica, Ricciardi, & Romano, 2017).

Although the rules enacted regarding gluten labeling have provided useful guidance, the lack of standardized testing methods have driven a demand for new gluten detection solutions (Do, Khuda, & Sharma, 2018). The enzyme-linked immunosorbent assay (ELISA) is often the laboratory method of choice as it can offer high gluten detection specificity and sensitivities with some quantitative measure (Schubert-Ullrich et al., 2009). Apart from the analytical variability of ELISA methods, gluten test results are impacted by the choice of antibodies, sampling

* Corresponding author.
E-mail address: Robert.hnasko@ars.usda.gov (R.M. Hnasko).

https://doi.org/10.1016/j.foodchem.2021.129514
Received 24 September 2020; Received in revised form 27 January 2021; Accepted 28 February 2021
Available online 13 March 2021

methodology, the complexity of food matrix and food processing procedures (Garcia, Llorente, Hernando, Kieffer, Wieser, & Mendez, 2005; Khuda et al., 2012).

The intention of gluten testing is to minimize the risk of unwanted gluten contamination of a food product. Toward that aim, we report on a new cohort of anti-gliadin monoclonal antibodies and their application in immunoassays for gluten detection. To achieve the need for robust testing from food production to consumption, we describe a threshold-based lateral flow immunoassay (LFIA) suitable for rapid detection of gluten from foods. To simplify testing we engineered a disposable, easy-to-use and traceable biosensor platform to facilitate gluten detection by inexpensive LFIA for industry and consumers from the farm to the fork.

2. Material methods

2.1. Immunization

An ethanol standard of wheat gliadin (Fitzgerald Industries, MA; 30R-3098) was used to create an immunogen with Freund's adjuvant system at 1 mg/mL. Female Balb/cByJ mice (Jackson Laboratory, ME) at 6 weeks of age were immunized by intraperitoneal injection (100 μL) with Freund's complete adjuvant and boost immunizations performed every 10–15 d with Freund's incomplete adjuvant. After the third boost, mouse sera were collected and antibody titers against gliadin proteins evaluated by indirect ELISA (see below). Mice with high antibody titers received a final boost without adjuvant and after 3 d were sacrificed and splenocytes harvested for cell fusion. All animal procedures where approved by the ARS-IACUC committee.

2.2. Cell fusions

The application of hybridoma technology for production of monoclonal antibodies was performed as previously described with some modifications (Hnasko & Stanker, 2015). Briefly, mouse splenocytes were prepared for cell fusion by passing through a wire sieve, red blood cells were lysed and intact cells collected following Histopaque-1077 cell isolation (Sigma, MO). Prior to fusion, all cells were subject to a cell dissociation buffer (Accumax; Innovative Cell Tech., CA) and passed through a 100 μm cell strainer with cell counting performed using a Scepter 60 μm tip (Millipore, MA). Myeloma cell lines (SP2/0 or P3X ARS subclones) were used as cell fusion partner and chemical fusion performed in serum-free media at a ratio of 4:1 (splenocyte:myeloma) using 3,000–3,700 MW polyethylene glycol (Sigma; P2906). Fused cells where diluted into complete IMDM cell culture media (see below) and incubated in T175 flasks at 37° C and 5% CO_2. After 3 d hybrid cells were subject to Histopaque-1077 isolation and diluted in complete IMDM for plating in 96-well cell culture plates or frozen in 10% dimethyl sulfoxide (DMSO) for liquid nitrogen storage and recall. Complete IMDM: Iscove's Modified Dulbecco's Medium (Gibco) was supplemented with 1) glutamax, 2) 25 mM HEPES, 3) sodium bicarbonate (3.024 g/L), 4) 10% heat-inactivated fetal bovine serum (FBS), 5) sodium pyruvate, 6) ITSE (InVitria, CO), 7) MEM vitamins, 8) 10% macrophage conditioned media (Hnasko, Lin, Stanker, & McGarvey, 2018), 9) Y-27632 (Selleck Chemicals; 10 μM) and 10) HAT (aminopterin) or HT (no aminopterin).

2.3. Hybridoma cell lines

Hybridoma cells were grown in microplates until visible colony formation (7–10 d). Primary screening for production of anti-gliadin antibodies were performed with culture media using high-throughput ELISA detection methodologies (see below). Cells from culture wells with positive anti-gliadin activity were transferred to 24-well plates and after 3 d of cell expansion culture media were evaluated for gliadin binding by ELISA. Cells from culture wells with anti-gliadin activity were subject to limiting dilution with HT replacing HAT in the complete IMDM. Secondary screening of sub-cloned hybridoma cells were evaluated by ELISA and the process continued until stable clonal cell lines producing anti-gliadin MAb were established. Final hybridoma cell lines were frozen in 10% DMSO and stored in liquid nitrogen with recall viability confirmed.

2.4. Monoclonal antibodies

Hybridoma clones obtained by limiting dilution were sub-cloned a final time in soft agar and expanded in cell culture flasks (IMDM with 10% FBS). Monoclonal antibodies were purified from culture media using protein-G HiTrap columns (GE Healthcare) by FPLC at neutral pH and bound antibodies were eluted with a 0.2 M glycine buffer (pH 2.3) as a single protein peak (280 nm UV) of 3 mL and subject to dialysis (20 K MW cut-off) in 20 mM PB pH 7.2. Antibody concentrations were determined by BCA assay using a BSA standard. Antibody isotypes were determined using Isostrips (Roche) and all reported in this manuscript were IgG1 subclass with kappa light chains.

2.5. ELISA assays

All ELISA assays used high-binding 96-well microplates (Greiner Bio-One LUMITRAC) and were performed at room temperature as previously described (Hnasko, 2015). Initial protein immobilization to plate surface was performed in 0.2 M carbonate-bicarbonate buffer (pH 9.4) for 1 h. Tris-buffered saline (pH 7.2) with 0.1% Tween-20 (TBST) was used for all wash steps, dilutions and blocking was performed with 10% non-fat dry milk (NFDM) for 0.5 h. Horseradish peroxidase (HRP) conjugates were used with a chemiluminescent substrate (Neogen, MI; ECL ultra) and detection with a Victor X3 plate reader (Perkin-Elmer) was reported as counts per second (CPS). Direct ELISA were performed using primary HRP-conjugated MAbs at 5 μg/mL in TBST as reporter (Lightning-link HRP; Innova Biosciences, UK) and indirect ELISA using a gt-anti-mo-gamma chain-HRP secondary antibody (0.2 μg/mL; Sigma) in TBST for 1 h. Direct ELISA data are reported as the MEAN CPS ± SEM (N = 3) with non-linear four parameter logistic curve fitting. Capture ELISA were performed using microplate immobilized gt-anti-mo-Fc (10 μg/mL; Jackson ImmunoResearch), capture of primary MAbs at 10 μg/mL, biotinylated gliadin (NHS-Btn-PEG4; Thermo Fisher) and avidin-HRP reporter (Sigma; A7419) with data reported as the MEAN CPS ± SEM (N = 4). Sandwich ELISA were performed by direct immobilization of the primary capture MAb (5 μg/mL) to the microplate and chemiluminescent detection via direct HRP-conjugated secondary MAb (3 μg/mL). Data is expressed a the MEAN CPS ± SEM (N = 4) and non-linear regression (four parameter logistic curve) performed ($R^2 = 0.99$) on a wheat dilution series. Sandwich ELISA performed on alcohol extracts of various grains (12 μg/mL) are reported as MEAN CPS ± SEM (N = 4) and *t*-test performed against assay background with statistical significance $p < 0.001$.

2.6. Western blot

Western blotting was performed as previously described (Hnasko & Hnasko, 2015). Briefly, an alcohol extract of wheat flour was heat denatured in LDS buffer and 2.4 μg of protein was separated on 4–12% BIS-TRIS gels in MOPS buffer by electrophoresis. Reduced samples (+) where denatured in LDS with 0.1 M DTT. A visual dual-color protein standard (BioRad, CA) was used to determine molecular weight (kDa). Separated proteins were transferred to nitrocellulose membranes, washed in TBST, blocked in 10% NFDM and incubated with protein-G purified MAb at 5 μg/mL then a gt-anti-mo (H + L) IgG-HRP conjugate (Sigma). Antibody binding to protein bands were resolved after 1 min using enhanced chemiluminescent substrate (Pierce; Supersignal picoECL) and images taken after 2 min using an AlphaInnotech ChemiDoc HD system. Alcohol extracts of an all-purpose and bread wheat flour (10 μg) were separated as described above and gel stained with Coomassie blue (Instant*Blue*; Sigma).

2.7. Antibody binding to gliadin peptides

Wheat alpha-gliadin protein sequences (Triticum *aestivum*) were aligned and a representative sequence was defined for use in the construction of overlapping peptides (see Supplemental Table 1 and Table 2). Peptides of 15-amino acids with 5-amino acid overlaps were synthesized with a *N*-terminal biotin, an Ahx spacer and C-terminal amidation, desalted and dissolved in DMSO (20 μg/mL). Peptides were diluted in TBST (2 μg/mL) for binding to avidin coated (2 μg/mL) 96-well microplates. Plates were blocked with 10% NFDM and incubated with MAb at 3 μg/mL in TBST then a gt-anti-mo-gamma chain-HRP (1 μg/mL) and ECL substrate (Neogen). Chemiluminescent detection was reported using a Victor X3 luminometer (0.2 *sec*/well) and expressed as CPS. Relative binding of antibodies were plotted and peptide binding evaluated for each MAb. A synthetic 33-mer peptide representing an allergenic alpha-gliadin motif (*N*-btn-ahx-LQLQPFPQPQLPYPQPQL-PYPQPQLPYPQPQPF) was also generated and binding of each MAb to this peptide evaluated (Cebolla, Moreno, Coto, & Sousa, 2018). The addition of a non-gliadin peptide or buffer alone were included as negative controls to establish assay background. Each assay was performed at least three times and data are representative of assay results (Supplemental Fig. S2). MAb peptide binding was subject to multiple sequence alignment (CLUSTAL Omega) and consensus binding sequence identified and aligned relative to alpha-gliadin sequences accession no. AAA34278 and AAA17741 (GenBank).

2.8. Flour extraction

Milled flours were obtained from a local grocer and included the following: 1) Bread wheat (hard Red; UPC 7101204105), 2) Whole wheat (hard Red; UPC 7101205050), 3) All-purpose wheat (hard Red; UPC 7101201050), 4) Pastry wheat (soft white; UPC 9948241830), 5) Rye (whole grain; UPC 3997800313), 6) Barley (stone ground; UPC 3997800301), 7) Oat (whole grain; UPC 3997800311), 8) Sorghum (gluten-free; UPC 3997800642), 9) Corn meal (stone ground; UPC 3997800303) and 10) peanut meal (defatted BRC262R; Sigma). Flours were weighed on an analytical scale to 100 mg dry weight and transferred into a 15 mL conical tube containing 4 mL of either 70% ethanol or 0.2 M phosphate buffer (pH 7.2) with 1% Triton-X 100. Samples were vortexed for 10 *sec* then incubated at room temperature for 5 min (wt/vol = 25 mg/mL). Hydrated flours were then subject to centrifugation at 15,000 × g for 10 min at 4° C. Flour supernatants were passed through a 0.2 μm PTFE filter and protein concentrations were determined by BCA assay. Efficiency of protein extraction ranged from 0.4 to 1.9 mg/mL.

2.9. Lateral flow test strip construction

The production of lateral flow test strips was performed as previously described (Bever, Adams, Hnasko, Cheng, & Stanker, 2020; Ching, He, Stanker, Lin, McGarvey, & Hnasko, 2015; Ching, Lin, McGarvey, Stanker, & Hnasko, 2012; Hnasko, Lin, & McGarvey, 2019) with some modifications. The 14G3 MAb was striped at 2.3 mg/mL in 20 mM PB (pH 7.2) with 1% HPLC-grade MeOH on RP immunopore membrane (GE Whatman) using a BioDot XYZ platform and biojet dispenser (1.25 μL/cm, 50 nL drops) at a test line (T). A dnk-anti-mo H + L chain IgG with minimal species cross reactivity (Jackson ImmunoResearch) was striped at 1 mg/mL at a control line (C). Membranes were dried in a convection oven 30 min at 37° C then blocked in 0.1% PVP-40 in water (polyvinylpyrrolidone mean MW = 40,000; Sigma) by submersion for 30 min at room temperature then washed in ddH20 three times and dried again at 37° C for 1 h. Membranes were stored at room temperature desiccated (<5% humidity) until assembly. The 8F3 MAb was conjugated to 15OD 40 nm gold sol (BioAssay Works, MD) adjusted to pH 8.2. Final 8F3 gold conjugate was 12OD with 1% trehalose (Sigma) and dispensed (4 × 1 mm offset) on a glass fiber pad (Millipore; G041) using an AirJet attached to the BioDot XYZ platform (5 μL/cm at 40 mm/s). The pads were dried at 37° C in an oven for 1 h and stored desiccated.

Test strip assembly was performed using a batch laminating system (BioDot LM5000) on a scored plastic backed adhesive card (60 × 300 mm, DCN, CA; MIB-020) with nitrocellulose RP membrane overlapped ~ 2 mm with the conjugate release pad followed by a Fusion 5 (GE Healthcare; 8151–9915) sample pad placed at the bottom of the card and covering the conjugate release pad. CF6 absorbent pad (GE Healthcare; 8166–2250) was placed at the top of the card with ~ 2 mm overlap of the nitrocellulose. Assembled cards were cut into 4.5 mm test strips using a guillotine cutter (BioDot CM4000). Test strips were placed in 2-part plastic housings or inserted into biosensor assemblies (see below). Complete test strips were stored desiccated and protected from light at room temperature.

2.10. Digital interrogation of gluten lateral flow tests

A HRDR-200 Smartphone reader (Holomic LLC., CA) was calibrated per manufacture instructions for evaluation of test strips housed in a two-part cassette using a gold reporter with a single test line (T) and control line (C). The integrated mean density was determined for each sample test line (N = 5) from a wheat dilution series then the MEAN ± standard deviation analyzed by nonlinear regression (four parameter logistic curve; $R^2 = 0.99$). The average coefficient of variation (CV) across the dilution series for the test strips was 12.9%.

2.11. Food sampling methodology

Food substrates obtained from a local grocer were weighed on an analytic scale and material transferred to 5 mL round bottom tubes containing 4 mL of 0.2 M phosphate buffer with 1% Triton-X 100 (pH 7.2). Tubes were inverted 3 × to hydrate and mix the food, then allowed to sit at room temperature for ~ 1 min. Samples of 100 μL were transferred to the sample pad of a gluten test strip and timed for 90 *sec*. Photographs were taken using a cell phone under white light after a total of 3 min and nominal data scored as positive (visible T and C lines = POS), negative (visible C line only = NEG), or fail (no visible C line = FAIL). Each food was tested with 3–5 independent samples. If the test result was negative a wheat gliadin spike of ≤ 20 μg/mL was added to the hydrated food and used to determine the impact of the food substrate on the test result.

2.12. Biosensor design and build

Autodesk Fusion 360 CAD software was used to design parts and 3D Sprint software used for printing on a ProJet MJP2500 Plus 3D printer (3D Systems, SC). VisiJet M2R plastic was used in conjunction with VisiJet M2 SUP material (3D Systems) to build the biosensor parts: 1) sampling cap, 2) liquid cartridge and 3) biosensor housing (see Fig. 5). Support wax was removed after printing using MJP EasyClean system with a steam bath followed by a hot mineral oil dip with a final soapy water wash before air drying. This process resulted in high resolution, waterproof parts that were used to assemble biosensors for use with lateral flow test strips and liquid filled cartridge-cap assemblies. More biosensor details can be found in U.S patent application serial No. 16/444,235.

3. Results and discussion

3.1. MAb binding to a wheat gliadin fraction by Western blot

Western blot analysis of a wheat prolamin fraction is consistent with MAb binding gliadin proteins (Fig. 1B). We compare MAb protein binding after heat denaturation and disulfide reduction. At the resolution of this technique, we observe a MAb binding pattern consistent with that of 30–50 kDa S-rich gliadins (Balakireva et al., 2016). The 18B10 and 2G10 MAbs bind poorly to heat denatured protein but binding is

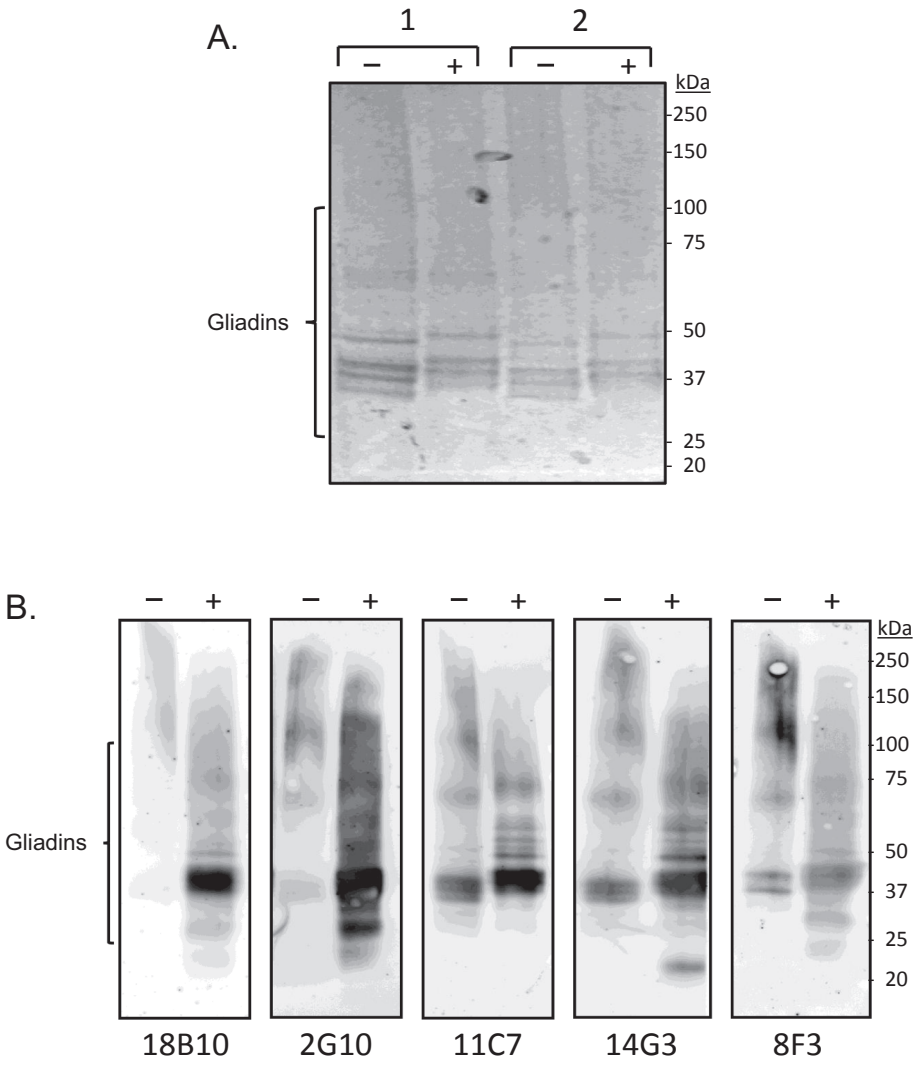

Fig. 1. Detection of wheat gliadin proteins by Western blot. An alcohol extract of wheat flour was heat denatured and subject to SDS-PAGE with (+) or without (-) 0.1 M DTT. A Coomassie stained gel (Panel A) shows predominant proteins from 10 μg of (1) wheat bread flour and (2) and all-purpose flour with the region containing gliadin proteins indicated (25–100 kDa). Western blotting (Panel B) with chemiluminescent detection was used to evaluate MAb binding to gliadin proteins from 2.4 μg of wheat flour extract.

enhanced following disulfide reduction. This suggests the binding epitopes of these MAbs are partially masked by these secondary structures, at least under heat denatured conditions. The 11C7, 14G3 and 8F3 MAbs binding is near equivalent to the heat denatured and disulfide reduced gliadins. The disruption of the disulfide bonds results in small MW band shifts associated with the disruption of inter- and intra-molecular disulfide bonds. A Coomassie stained gel (Fig. 1A) shows the predominant gliadin protein bands from ethanol extracts of all-purpose and wheat bread flours. A higher resolution technique, such as 2D acid PAGE (Vensel, Tanaka, & Altenbach, 2014), using genetically defined wheat strains should help elucidate the specific binding of each MAb to known protein sequences and corroborate genetic expression data. These MAbs and those from our larger cohort will be useful tools in the proteomic analysis of prolamin expression from genetic wheat variants and other grains.

3.2. MAb binding to gliadin peptide sequences

To identify MAb binding epitopes, a series (N = 29) of biotinylated 15-amino acid peptides representing alpha-gliadin were immobilized on avidin-coated microplates (Supplemental Table 2). Relative MAb binding to each peptide by ELISA was plotted (Supplemental Fig. S2) and all but the 8F3 MAb report strong selective peptide binding. Supplemental Table 1 reports the linear amino acid sequence used to construct the mapping peptides, with relevant peptide binding for each MAb indicated in bold text, and the predicted MAb binding epitope (highlight) aligned with wheat alpha-gliadin sequences.

Only the 18B10 MAb bound the 33-mer alpha-gliadin peptide and together with the broader peptide binding data suggests the PYPQ sequence is important in 18B10 antibody binding. The 2G10 MAb peptide binding suggests a QPYPQ binding epitope and no binding to the 33-mer peptide denotes some importance to the initial glutamine (Q) residue as the 33-mer peptide contains a leucine (L)PYPQ repeat. The importance of these putative MAb binding epitopes are underscored by their occurrence in immunodominant gliadin motifs associated with celiac disease (Bromilow et al., 2017). Moreover, the 18B10 and 2G10 MAb binding motifs differ from those reported for the anti-gluten R5 and G12 MAb used in many commercial gluten tests (Kahlenberg et al., 2006; Morón et al., 2008). Although both MAbs solution capture wheat gliadin, neither was particularly effective as a partner when paired in sandwich ELISA or LFIA with MAbs from our antibody cohort (data not shown). It will be of interest to evaluate the capability of both the 18B10 and 2G10 MAbs for gluten detection when paired with either the R5 or G12 anti-gluten MAbs. The 11C7 MAb bound only one peptide with the core sequence AMCNV in the C-terminal region of gliadin. Interestingly, the presence of a cysteine residue in this motif and any associated disulfide linkage (Lutz, Wieser, & Koehler, 2012) is neither required nor inhibits 11C7 MAb binding to gliadin. Some binding to the overlapping C-terminal peptide suggests a contribution of the YIPPY sequence in MAb binding that may account for this observation. Direct ELISA

binding of these three MAbs to a dilution series of a wheat gliadin extract is reported in Supplemental Fig. S1 with non-linear curve fitting. The EC50 for wheat gliadin detection with the 2G10 MAb is 0.44 μg/mL (Fig. S1A), 11C7 MAb is 0.37 μg/mL (**Fig. S1B**) and 18B10 MAb is 0.13 μg/mL (Fig. S1C).

The peptide binding data for the 14G3 and 8F3 MAbs suggests they bind more complex discontinuous epitopes. The 14G3 MAb binds denatured and reduced gliadins by Western blot and three non-overlapping linear peptides with core sequences QQQQF, PQQPY and VSFQQ, but no clear consensus sequence. These data argue the 14G3 MAb can bind linear gliadin motifs, but the native binding epitope likely involves a more complex interaction of discontinuous gliadin sequences. The observation that 14G3 can self-pair (data not shown) may reflect this dual binding property and the repeat occurrence of core peptide motifs in gliadin proteins. The 8F3 MAb can bind denatured and reduced gliadin proteins, but no convincing epitope emerged from our peptide binding data suggesting interaction with an unrepresented peptide sequence or a conformational gliadin epitope.

3.3. MAb performance in capture and sandwich ELISA

Antibodies that bind linear epitopes tend to perform well in immunoassay techniques that detect denatured or immobilized proteins. Solution capture of proteins in native conformation often rely on antibodies that bind more complex discontinuous epitopes. The goal of this work was to generate MAbs that perform in a LFIA format for the detection of gluten from foods. To achieve this aim, we required a pair of MAbs that each bind to unique or redundant epitope in the gluten protein that are capable of solution capture. The capture ELISA is useful assay as both a selective hybridoma screening tool, but also as a method to narrow down the pool of isolated MAbs for evaluation as functional pairs that can perform in a sandwich ELISA. The 14G3 and 8F3 MAbs were immobilized by their Fc-domains and binding determined for a dilution series of biotinylated wheat gliadin (Supplemental Fig. S1). These two MAbs capture the biotinylated gliadin with good linearity and high sensitivity (50 ng/mL $p < 0.05$).

The development of a sandwich ELISA (sELISA) requires MAb properties that include binding of an analyte in solution and the coordinated binding of a MAb pair. The optimal MAb pair for construction of a sELISA for gluten detection was determined to be the 14G3 MAb used for the analyte capture and the 8F3 used as a reporter conjugate. This sELISA was used for the detection of a wheat gliadin dilution series (Fig. 2A) and the data fits a non-linear regression curve with an EC50 of 4.4 μg/mL and a detection limit of 100 ng/mL ($p < 0.001$). The linearity of the assay was optimal between 20 and 5 μg/mL ($R^2 = 0.9982$) but could be extended from 20 to 0.1 μg/mL ($R^2 = 0.8716$). To determine the specificity of the sELISA we evaluated a variety of milled flour and meal extracts (Fig. 2B). Gluten was detected in all wheat flours (hard red and soft white), rye and barley extracts ($p < 0.001$) but was undetectable in oat, sorghum, corn and peanut meal (12 μg/mL).

3.4. Gluten LFIA performance

Antibodies used in the development of a LFIA require rapid binding kinetics and must retain their functional binding after immobilization and desiccation. The optimal antibodies determined for the development of a gluten LFIA were the 14G3 MAb immobilized at test line (T) and the 8F3 MAb conjugated to a gold reporter for visual color detection (Fig. 3). A dilution series of wheat gliadin was evaluated and visual detection was reported at concentrations between 0.5 and 500 μg/mL of gliadin in < 3 min with 100 μL (Fig. 3A). If the time of the LFIA was extended to 5 min, gliadin detection was reported at 150 ng/mL (Fig. 3B). The color intensity of the test line (T) peaked at ~ 30 μg/mL of gliadin, but positive test lines were visible across the entire gliadin dilution series even at very high concentrations. A short video showing real-time results of gliadin detection at 20 μg/mL in ~ 1.5 min with the

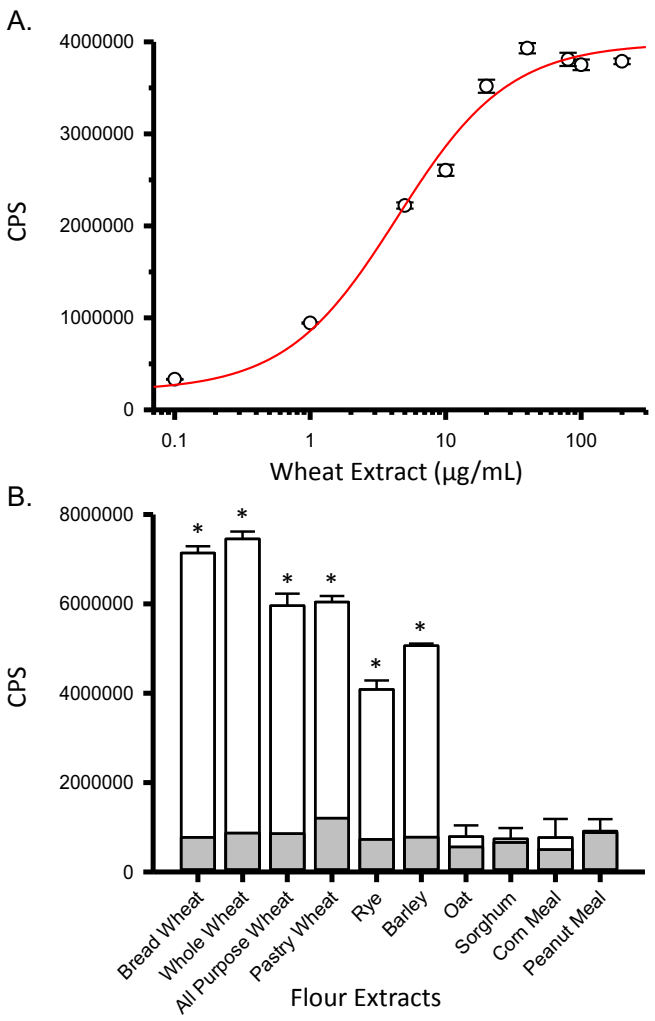

Fig. 2. Detection of wheat gluten by sandwich ELISA. The 14G3 MAb was immobilized as a capture reagent (5 μg/mL) and paired with the 8F3-HRP MAb conjugate (3 μg/mL) for chemiluminescent detection reported as MEAN ± SEM (N = 4) in counts per *sec* (CPS). Panel A. Detection of gluten in a dilution series of a wheat flour extract. The line plots the data using nonlinear regression (four parameter logistic curve, $R^2 = 0.99$). Panel B. Relative detection of gluten from alcohol extracts (12 μg/mL) of cereal grains and ground meals (open boxes) stacked with the MEAN of each assay background (filled box). Statistical significance (*) *t*-test $p < 0.001$.

LFIA is shown in Supplemental Video 1. A digital smartphone reader (HRDR-200) was used to interrogate results of LFIA test strips from a dilution series of a wheat extract (Fig. 4). The integrated mean density of each sample (N = 5) was determined at the test line (T) and plotted using a non-linear regression curve ($R^2 = 0.99$) reporting an EC50 for gluten detection of 1.11 μg/mL.

3.4.1. LFIA detection of gluten in grain flours

Flour extracts of wheat, rye and barley are gluten positive by LFIA at 50 μg/mL (<3 min) and negative for sorghum and peanut meal (Fig. 3C). However, at this protein concentration our LFIA reported a gluten positive test result for oats. The concentration of oat protein tested exceeds the threshold (2.5 ×) for gluten-free product and likely reflects the detection of residual gluten cross-contamination of oat product. To assess the impact of heat treatment on gluten detection we compared boiled and dry wheat pasta to that of gluten-free pasta with our LFIA (Fig. 3D). Simple weight to volume extraction was employed and both boiled and dry wheat pasta resulted in positive gluten detection and gluten-free pasta (corn and rice blend) was negative. A wheat gliadin

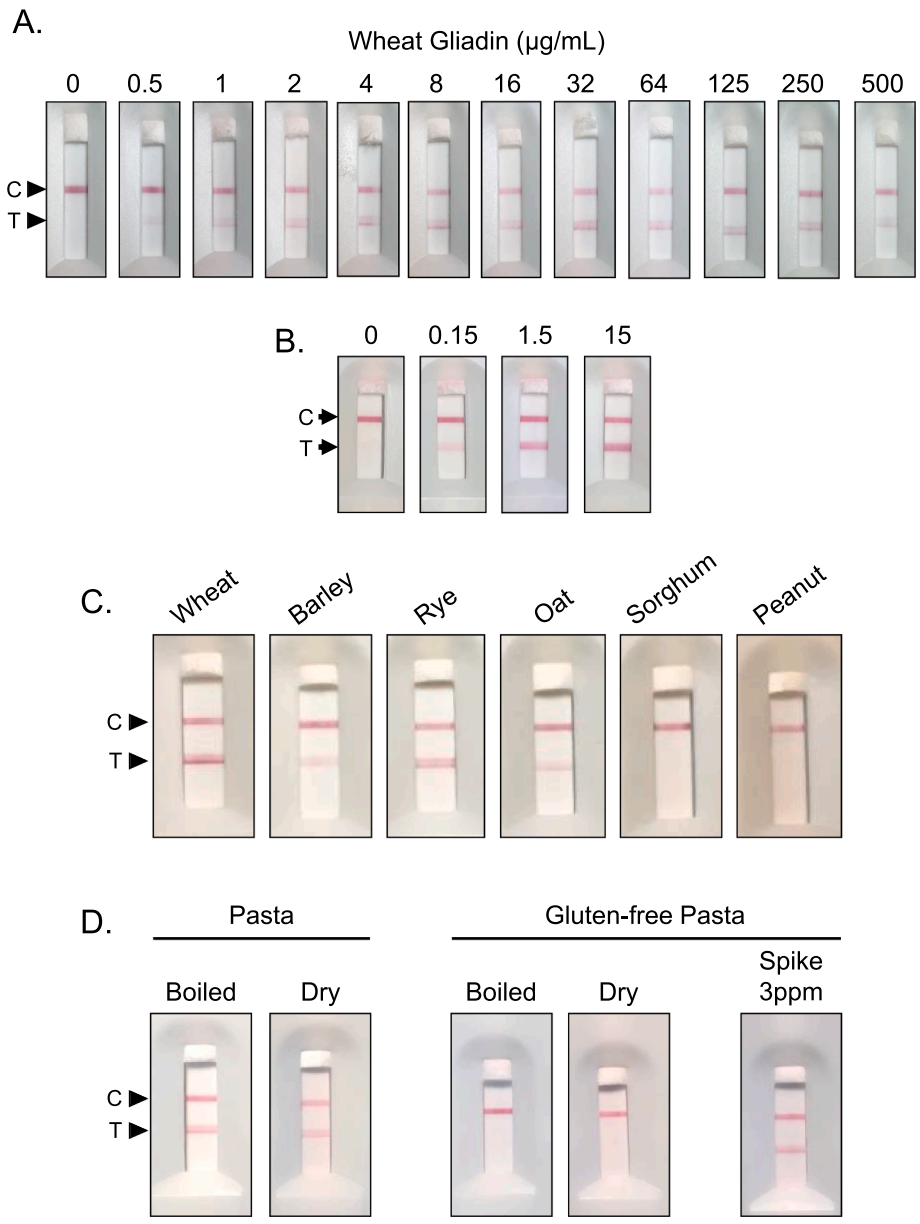

Fig. 3. Rapid and sensitive detection of gluten by LFIA. The 14G3 MAb was striped on nitrocellulose at a test line (T) and the 8F3 MAb conjugated to a 40 nm gold reporter and the LFIA was used to test a dilution series of wheat gliadin. A visible color band at the test line (T) was reported as a positive test result from 0.5 − 500 µg/mL of gliadin within a 3 min assay runtime (Panel A). When the assay runtime is extended to 5 min the detection of 150 ng/mL can be achieved (Panel B). Milled flour extracts (50 µg/mL) where evaluated for gluten detection by LFIA after 90 *sec* with representative examples shown in Panel C. Detection of gluten by LFIA from equivalent (wt/vol) wheat and gluten-free pasta are compared in Panel D as a dry or boiled product extract. A visible test (T) and control line (C) indicates a gluten positive test result. A negative test result is indicated by a visible control line (C) only. Images where taken using a cell phone camera with white light.

spike (3 µg/mL) was used to ensure there was no substrate interference with the gluten-free extract and resulted in a positive test result.

3.4.2. *LFIA detection of gluten in foods*

A nominal LFIA with broad gluten detection capability provides a user with a fast and portable measure of gluten in a food sample. Toward that aim, we constructed a gluten LFIA that would perform for both solid or liquid food substrates with passive extraction in a defined volume (4 mL) of buffer (0.2 M PB + 1% Triton-X 100 at pH 7.2) without the need for end-user dilution. The inclusion of 1% non-ionic detergent Triton-X 100 facilitates protein extraction and works as a surfactant. The addition of salt (<1M NaCl) has negligible impact on the performance of our gluten LFIA (data not shown). No alcohol is used and the sample buffer components are non-toxic. To overcome the challenges associated with material clogging and slow flow rates due to particulate food substrates, we utilized the fast-flowing hydrophilic Fusion 5 material as a sample pad. This material works effectively to filter and retain both large and small particles to maintain rapid capillary fluid flow between materials.

We chose a variety of foods for testing that included different textured solids and liquids along with those labeled gluten-free. Sample size reflect portions (0.3–2.5 g) that a user would fit in a 25 mm tube opening filled with 4 mL of buffer. Foods were tested and gluten determined with representative examples of test strips shown to illustrate the test result and the effective filtration of the sample pad for food particulates (Supplemental Fig. S4). A test result was determined after 3 min by visual scoring and any resolving test line > 3 min would be considered negative in this assay as < 0.5 µg/mL. Table 1 reports the food tested, if wheat was declared on the package label (Yes or No), weight or volume of food sampled and a positive (POS) or negative (NEG) test result. Five independent tests were performed for each food, visually scored (POS, NEG or FAIL) and photographed using a mobile phone camera under white light.

In general, gluten detection by our LFIA accurately reported food labeling. Foods containing oats resulted in a positive gluten test for some, but not all, gluten-free labeled product. These positive gluten test results for oat likely reflects cross-contamination of the product during production with gluten that exceeds the assay detection threshold (>0.5 µg/mL). Gluten was not detected in fermented wheat product (soy sauce) and this negative result was not due to substrate interference, suggesting fermentation disrupts the MAb binding epitopes. A wheat

Fig. 4. Digital reader interrogation of LFIA tests from a wheat extract dilution series. A Holomic HRDR-200 Smartphone reader was calibrated for evaluation of a gold reporter and the Integrated Mean Density determined for each sample (N = 5), then plotted as the MEAN ± standard deviation of the test line (T). Nonlinear regression (four parameter logistic curve, $R^2 = 0.99$) is plotted as a line. The average coefficient of variation (CV) = 12.9%.

gluten spike (20 µg/mL) was used to rule out food matrix interference on all negative test results. The detection threshold of the of gluten LFIA assay can be reduced by altering the MAb concentrations or sensitivity increased by use of alternate molecular reporters or detection chemistries.

3.5. LFIA test strip platform

The utility of a LFIA for detection of gluten would benefit from integration of sampling methodology and testing. Many LFIA are provided in a kit format with separate components for sample extraction and liquid transfer. This requires the user to conduct a multi-step process to perform a test. This added complexity can slow the testing process and increase user error. To overcome these challenges, we engineered a biosensor platform that simplifies the user experience and provides a plug-*n*-play flexibility to accommodate industry standard test strips and diverse sampling requirements (Fig. 5). It is a disposable device designed to simplify the testing process in a pocket-sized platform. It is traceable, requires limited training to perform, with results that are fast and actionable. Modular components are used to maintain needed separation of the dry (test strip) from the aqueous (sample buffer) components until testing is initiated by a user with a simple mechanical mechanism.

The platform consists of three disposable plastic components: 1) biosensor housing, 2) liquid cartridge and 3) sampling cap (Fig. 5A). The cartridge can be pre-filled with any compatible liquid sample buffer and is sealed with a cap. The cartridge has internal threads that accept a cap that integrates a sampling tool. The user gains access to the liquid buffer via the cap, adds a sample with the aid of the sampling tool and reseals the cartridge. The size of the cartridge opening and cap tool helps restrict user sample size and facilitates mixing when sealing. After mixing, the cartridge is inserted into the opening of the biosensor housing and the test is initiated by the user with a simple twist of the cartridge that breaks the frangible bottom with a spear located at the bottom of the biosensor housing (Fig. 5B). Some liquid from the cartridge is driven through a small restriction port that separate the test strip chamber from the cartridge chamber. Liquid contact with the test strip sample pad at the port initiates capillary fluid flow and the test begins. The test strip chamber uses a flexible plate to maintain contact between overlapping test strip materials that self-adjusts to different material thickness. The current design limits the release of solids and liquid from the sample cartridge preventing flooding of the test strip chamber and particulate clogging of the port opening. The liquid sample is delivered to the test strip by a continuous capillary draw until material saturation. Test results are visually interpreted at the result window and the device can be adapted for digital result interrogation and reporting. An example of the biosensor performance for the detection of < 20 µg/mL of wheat gluten in < 3 min is shown in Fig. 5D and Supplemental Video 2.

This biosensor design provides plug-*n*-play flexibility for most industry standard test strips. Customized buffer composition and sampling cap combinations can be used to meet most test requirements. Additional modules that link to the buffer cartridge have been engineered to perform more complex or sequential sampling methods (Fig. 5C). These modular components provide added flexibility to the platform to accommodate different assay requirements. Integration of the biosensor with a reader for digital interrogation of test lines will further simplify an end-user experience and provide traceable results with remote bioinformatics.

Table 1
Gluten LFIA test results from food products. Foods were weighed, or volume measured, then added directly to 4 mL of buffer for 1 min with sporadic mixing by hand. A volume of 100 µL was added to a LFIA test strip and gluten detection determined by visual observation after 3 min. Food package labeling of wheat is indicated as a yes (Y) or no (N) and test results reported as positive (POS) or negative (NEG). Each food substrate was evaluated from 5 independent samples for scoring. See Supplemental Fig. S2 for visual LFIA test results for foods A-L. Negative food substrates were spiked with a wheat gliadin extract (≤20 µg/mL) that all resulted in positive detection after spike.

	Food Substrate	Wheat Indicated	Buffer(4 mL)	Test Results
A	Wheat Bread	Y	0.9 g	POS
B	Gluten-free Bread	N	0.5 g	NEG
C	Corn Chips	Y	1.0 g	NEG
D	Wheat Thins	Y	1.0 g	POS
E	Gluten-free Lentil Chips	N	0.5 g	NEG
F	Rice Cracker	N	0.3 g	NEG
G	Gluten-free Oat Granola	N	1.5 g	POS
H	Gluten-free Oatmeal	N	0.5 g	POS
I	Gluten-free Tomato Soup	N	0.3 mL	NEG
J	Taco Seasoning	Y	0.5 g	POS
K	Bagel	Y	0.4 g	POS
L	Poultry Rub	N	0.5 g	POS
	Baguette	Y	0.3 g	POS
	Italian Dressing	N	0.5 mL	NEG
	Marinara Sauce	N	1.0 mL	NEG
	Soba Noodles	Y	0.5 g	POS
	Soy Sauce	Y	1.0 mL	NEG
	Gluten-free Teriyaki Sauce	N	0.5 mL	NEG
	Gluten-free Seasoned Crouton	N	0.5 g	NEG
	Pizza Crust	N	0.6 g	NEG
	Gluten-free Corn & Quinoa Pasta	N	0.6 g	NEG
	Gluten-free Brown Gravy Mix	N	0.6 g	NEG
	Gluten-free Cheddar Soup Mix	N	0.5 g	NEG
	Breaded Chicken Nuggets	Y	1.0 g	POS
	Gluten-free Cornstarch Calamari	N	1.0 g	NEG
	Gluten-free Sweet potato Ravioli	N	1.5 g	NEG
	Spaghetti & Meatballs Marinara	N	2.5 g	POS
	Spaghetti Pasta	Y	2.5 g	POS
	Gluten-free Pasta	N	2.5 g	NEG
	Gluten-free Thai Lime Rice	N	0.8 g	NEG
	Gluten-free Pumpkin Sauce	N	0.5 mL	NEG
	Gluten-free Tamari Soy Sauce	N	0.5 mL	NEG
	Gluten-free Pinto Bean Chips	N	0.8 g	NEG
	Chicken Noodle Soup	Y	0.5 mL	NEG
	Seasoned Almonds	N	1.0 g	NEG
	Gluten-free Vinaigrette	N	0.5 mL	NEG
	Nut Thins	N	1.0 g	NEG
	Gluten-free Chewy Granola Bar	N	1.5 g	NEG
	Ketchup	N	0.5 mL	NEG

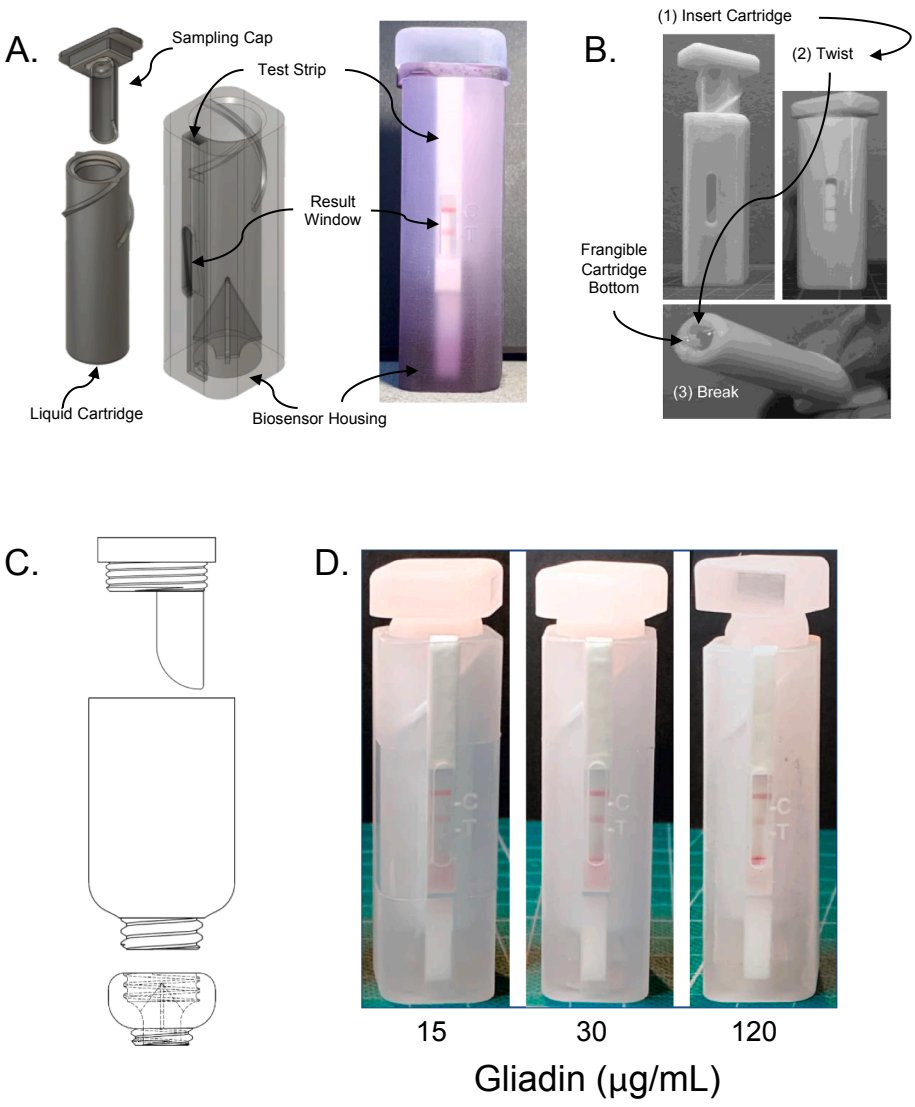

Fig. 5. Test strip biosensor design, function and performance. Three modular plastic components of a biosensor assembly 1) sampling cap, 2) liquid cartridge and 3) biosensor housing are shown graphically in Panel A next to a 3D-printed prototype showing the location of the test strip and result window. To perform a test. an end-user removes the sample cap from the liquid filled cartridge then adds a sample assisted by the integrated cap tool. The cartridge is resealed and agitated to facilitate analyte extraction. The test is started by the user after inserting the cartridge into the biosensor housing with a twist that results in the puncture of the frangible cartridge bottom by the inner spear of the biosensor housing (Panel B). Liquid from the cartridge moves into the biosensor housing, then through a small restrictor port into the test strip chamber where it contacts the sample pad of the test strip resulting in capillary fluid flow. The modular design of the platform allows for the interchange of cartridge-cap assemblies, test strips and expansion modules as depicted in Panel C to accommodate more complex sequential sampling procedures. The performance of the biosensor is illustrated in Panel D with a wheat dilution series and detection of gluten determined by a visible test line (T).

4. Conclusion

Gluten testing, as part of a food allergen management program, should provide a traceable and actionable measure of gluten in product. Testing should promote consumer trust and confidence by limiting risk of gluten contamination and reducing product recalls. The LFIA offers a low-cost alternative to conventional laboratory testing by changing where and by whom testing is performed at a cost that promotes an increase in the frequency of testing. In this manuscript we report on a new cohort of MAbs and their application in the detection of gluten by immunoassay. We developed a sensitive sELISA (LOD = 0.10 µg/mL) and rapid colorimetric LFIA (5 min; LOD = 0.15 µg/mL) for the detection of gluten in food products containing wheat, rye and barley.

In practice, food producers require a threshold-based gluten detection measure (<20 µg/mL) as a basis of gluten-free food labeling; whereas consumers may desire a much lower threshold to make informed food choices. A few gluten LFIA's have been commercialized to meet a growing demand from food producers for rapid and affordable test solutions (Lexhaller, Tompos, & Scherf, 2016). In supplemental Fig. S5 we compare the performance of our rapid LFIA (<5 min) to an existing commercial product that takes 22 min to perform. Most LFIA kits lack the necessary integration of test components and traceability for widespread adoption. Technological innovations that simplify and integrate LFIA testing have recently emerged to meet consumer demand for home gluten testing (Zhang et al., 2019).

To address these gaps in testing at the point of sample we introduce a portable biosensor to simplify gluten detection by LFIA from foods. This modular biosensor provides a flexible platform with broad LFIA applicability. This technology simplifies and integrates the steps needed for an end-user to perform a LFIA in the field with real-time actionable test results. The current LFIA biosensor design offers energy-independent visual test results in a traceable single-use platform. The increased use of a gluten LFIA, as a part of robust on-site food allergen testing program, will improved food transparency and bolster consumer confidence in food product choices.

CRediT authorship contribution statement

Robert M. Hnasko: Conceptualization, Investigation, Visualization, Validation, Supervision. **Eric S. Jackson:** Conceptualization, Investigation, Validation. **Alice V. Lin:** Investigation, Validation. **Ronald P. Haff:** Resources, Writing - review & editing. **Jeffery A. McGarvey:** Conceptualization, Writing - review & editing.

Declaration of Competing Interest

The authors declare that they have no known competing financial interests or personal relationships that could have appeared to influence the work reported in this paper.

Acknowledgements

This research was supported by the USDA-ARS National Programs in Food Safety (2030-42000-052) and Animal Health (2030-32000-010). The USDA is an equal opportunity provider and employer.

Appendix A. Supplementary data

Supplementary data to this article can be found online at https://doi.org/10.1016/j.foodchem.2021.129514.

References

Balakireva, A., & Zamyatnin, A. (2016). Properties of Gluten Intolerance: Gluten Structure, Evolution, Pathogenicity and Detoxification Capabilities. *Nutrients, 8*(10), 644. https://doi.org/10.3390/nu8100644.

Bever, C. S., Adams, C. A., Hnasko, R. M., Cheng, L. W., Stanker, L. H., & Soto-Blanco, B. (2020). Lateral flow immunoassay (LFIA) for the detection of lethal amatoxins from mushrooms. *PLoS One, 15*(4), e0231781. https://doi.org/10.1371/journal.pone.0231781.

Boyce, J. A., Assa'ad, A., Burks, A. W., Jones, S. M., Sampson, H. A., Wood, R. A., … Schwaninger, J. M. (2010). Guidelines for the Diagnosis and Management of Food Allergy in the United States: Summary of the NIAID-Sponsored Expert Panel Report. *J Allergy Clin Immunol, 126*(6), 1105–1118. https://doi.org/10.1016/j.jaci.2010.10.008.

Bromilow, S., Gethings, L. A., Buckley, M., Bromley, M., Shewry, P. R., Langridge, J. I., & Clare Mills, E. N. (2017). A curated gluten protein sequence database to support development of proteomics methods for determination of gluten in gluten-free foods. *J Proteomics, 163*, 67–75. https://doi.org/10.1016/j.jprot.2017.03.026.

Catassi, C., Bai, J., Bonaz, B., Bouma, G., Calabrò, A., Carroccio, A., … Fasano, A. (2013). Non-Celiac Gluten sensitivity: The new frontier of gluten related disorders. *Nutrients, 5*(10), 3839–3853. https://doi.org/10.3390/nu5103839.

Cebolla, Á., Moreno, M., Coto, L., & Sousa, C. (2018). Gluten Immunogenic Peptides as Standard for the Evaluation of Potential Harmful Prolamin Content in Food and Human Specimen. *Nutrients, 10*(12), 1927. https://doi.org/10.3390/nu10121927.

Ching, K. H., He, X., Stanker, L. H., Lin, A. V., McGarvey, J. A., & Hnasko, R. (2015). Detection of shiga toxins by lateral flow assay. *Toxins (Basel), 7*(4), 1163–1173. https://doi.org/10.3390/toxins7041163.

Ching, K. H., Lin, A., McGarvey, J. A., Stanker, L. H., & Hnasko, R. (2012). Rapid and selective detection of botulinum neurotoxin serotype-A and -B with a single immunochromatographic test strip. *J Immunol Methods, 380*(1–2), 23–29. https://doi.org/10.1016/j.jim.2012.03.008.

Delcour, J. A., Joye, I. J., Pareyt, B., Wilderjans, E., Brijs, K., & Lagrain, B. (2012). Wheat gluten functionality as a quality determinant in cereal-based food products. *Annu Rev Food Sci Technol, 3*(1), 469–492. https://doi.org/10.1146/annurev-food-022811-101303.

Diaz-Amigo, C., & Popping, B. (2012). Gluten and gluten-free: Issues and considerations of labeling regulations, detection methods, and assay validation. *J AOAC Int, 95*(2), 337–348. https://doi.org/10.5740/jaoacint.sge_diaz-amigo.

Do, A. B., Khuda, S. E., & Sharma, G. M. (2018). Undeclared Food Allergens and Gluten in Commercial Food Products Analyzed by ELISA. *J AOAC Int, 101*(1), 23–35. https://doi.org/10.5740/jaoacint.17-0384.

Fierro, V., Di Girolamo, F., Marzano, V., Dahdah, L., & Mennini, M. (2017). Food labeling issues in patients with severe food allergies: Solving a hamlet-like doubt. *Curr Opin Allergy Clin Immunol, 17*(3), 204–211. https://doi.org/10.1097/ACI.0000000000000362.

Garcia, E., Llorente, M., Hernando, A., Kieffer, R., Wieser, H., & Mendez, E. (2005). Development of a general procedure for complete extraction of gliadins for heat processed and unheated foods. *Eur J Gastroenterol Hepatol, 17*(5), 529–539. https://doi.org/10.1097/00042737-200505000-00010.

Gendel, S. M. (2013). The regulatory challenge of food allergens. *J Agric Food Chem, 61*(24), 5634–5637. https://doi.org/10.1021/jf302539a.

Gendel, S. M., & Zhu, J. (2013). Analysis of U.S. Food and Drug Administration food allergen recalls after implementation of the food allergen labeling and consumer protection act. *J Food Prot, 76*(11), 1933–1938. https://doi.org/10.4315/0362-028X.JFP-13-171.

Gupta, R., Holdford, D., Bilaver, L., Dyer, A., Holl, J. L., & Meltzer, D. (2013). The economic impact of childhood food allergy in the United States. *JAMA Pediatr, 167*(11), 1026–1031. https://doi.org/10.1001/jamapediatrics.2013.2376.

Gupta, R. S., Warren, C. M., Smith, B. M., Jiang, J., Blumenstock, J. A., Davis, M. M., … Nadeau, K. C. (2019). Prevalence and Severity of Food Allergies Among US Adults. *JAMA Netw Open, 2*(1), e185630. https://doi.org/10.1001/jamanetworkopen.2018.5630.

Hnasko, R. (2015). *ELISA: Methods Mol Biol, 1318*. Humana Press.

Hnasko, R., Lin, A. V., & McGarvey, J. A. (2019). Rapid Detection of Staphylococcal Enterotoxin-B by Lateral Flow Assay. *Monoclon Antib Immunodiagn Immunother, 38*(5), 209–212. https://doi.org/10.1089/mab.2019.0028.

Hnasko, R., Lin, A. V., Stanker, L., & McGarvey, J. (2018). A Bioassay for Optimization of Macrophage-Conditioned Medium as a Culture Supplement to Promote Hybridoma Cell Survival and Growth. *Monoclon Antib Immunodiagn Immunother, 37*(3), 126–133. https://doi.org/10.1089/mab.2018.0008.

Hnasko, R. M., & Stanker, L. H. (2015). Hybridoma Technology. *Methods Mol Biol, 1318*, 15–28. https://doi.org/10.1007/978-1-4939-2742-5_2.

Hnasko, T. S., & Hnasko, R. M. (2015). The Western Blot. *Methods Mol Biol, 1318*, 87–96. https://doi.org/10.1007/978-1-4939-2742-5_9.

Kahlenberg, F., Sanchez, D., Lachmann, I., Tuckova, L., Tlaskalova, H., Mendez, E., & Mothes, T. (2006). Monoclonal antibody R5 for detection of putatively coeliac-toxic glaidin peptides. *Eur Food Res Technol, 222*, 78–82. https://doi.org/10.1007/s00217-005-0100-4.

Khuda, S., Slate, A., Pereira, M., Al-Taher, F., Jackson, L., Diaz-Amigo, C., … Williams, K. M. (2012). Effect of processing on recovery and variability associated with immunochemical analytical methods for multiple allergens in a single matrix: Sugar cookies. *J Agric Food Chem, 60*(17), 4195–4203. https://doi.org/10.1021/jf3001839.

Kulis, M., Wright, B. L., Jones, S. M., & Burks, A. W. (2015). Diagnosis, management, and investigational therapies for food allergies. *Gastroenterology, 148*(6), 1132–1142. https://doi.org/10.1053/j.gastro.2015.01.034.

Lexhaller, B., Tompos, C., & Scherf, K. A. (2016). Comparative analysis of prolamin and glutelin fractions from wheat, rye, and barley with five sandwich ELISA test kits. *Anal Bioanal Chem, 408*(22), 6093–6104. https://doi.org/10.1007/s00216-016-9721-7.

Lutz, E., Wieser, H., & Koehler, P. (2012). Identification of disulfide bonds in wheat gluten proteins by means of mass spectrometry/electron transfer dissociation. *J Agric Food Chem, 60*(14), 3708–3716. https://doi.org/10.1021/jf204973u.

Moron, B., Bethune, M. T., Comino, I., Manyani, H., Ferragud, M., Lopez, M. C., & Sousa, C. (2008). Toward the assessment of food toxicity for celiac patients: characterization of monoclonal antibodies to a main immunogenic gluten peptide. *PLoS One, 3*(5). https://doi.org/10.1371/journal.pone.0002294.

Sathe, S. K., Liu, C., & Zaffran, V. D. (2016). Food Allergy. *Annu Rev Food Sci Technol, 7*(1), 191–220. https://doi.org/10.1146/annurev-food-041715-033308.

Schubert-Ullrich, P., Rudolf, J., Ansari, P., Galler, B., Fuhrer, M., Molinelli, A., & Baumgartner, S. (2009). Commercialized rapid immunoanalytical tests for determination of allergenic food proteins: An overview. *Anal Bioanal Chem, 395*(1), 69–81. https://doi.org/10.1007/s00216-009-2715-y.

Shewry, P. (2019). What Is Gluten-Why Is It Special? *Front Nutr, 6*, 101. https://doi.org/10.3389/fnut.2019.00101.

Shewry, P. R. (2009). Wheat. *J Exp Bot, 60*(6), 1537–1553. https://doi.org/10.1093/jxb/erp058.

Shewry, P. R., Halford, N. G., Belton, P. S., & Tatham, A. S. (2002). The structure and properties of gluten: An elastic protein from wheat grain. *Philos Trans R Soc Lond B Biol Sci, 357*(1418), 133–142. https://doi.org/10.1098/rstb.2001.1024.

Shewry, P. R., & Hey, S. J. (2015). The contribution of wheat to human diet and health. *Food Energy Secur, 4*(3), 178–202. https://doi.org/10.1002/fes3.64.

Spotz, K. (2018). Allergens: An Enhanced Focus. *J AOAC Int, 101*(1), 56–59. https://doi.org/10.5740/jaoacint.17-0435.

Valenti, S., Corica, D., Ricciardi, L., & Romano, C. (2017). Gluten-related disorders: Certainties, questions and doubts. *Ann Med, 49*(7), 569–581. https://doi.org/10.1080/07853890.2017.1325968.

Vensel, W. H., Tanaka, C. K., & Altenbach, S. B. (2014). Protein composition of wheat gluten polymer fractions determined by quantitative two-dimensional gel electrophoresis and tandem mass spectrometry. *Proteome Sci, 12*(1), 8. https://doi.org/10.1186/1477-5956-12-8.

Wang, D., Li, F., Cao, S., & Zhang, K. (2020). Genomic and functional genomics analyses of gluten proteins and prospect for simultaneous improvement of end-use and health-related traits in wheat. *Theor Appl Genet, 133*(5), 1521–1539. https://doi.org/10.1007/s00122-020-03557-5.

Wieser, H. (2007). Chemistry of gluten proteins. *Food Microbiol, 24*(2), 115–119. https://doi.org/10.1016/j.fm.2006.07.004.

Zhang, J., Portela, S. B., Horrell, J. B., Leung, A., Weitmann, D. R., Artiuch, J. B., … Yates, S. N. (2019). An integrated, accurate, rapid, and economical handheld consumer gluten detector. *Food Chem, 275*, 446–456. https://doi.org/10.1016/j.foodchem.2018.08.117.